Raja N.L. Khan Women's College

International Research Journal of Basic and Applied Sciences 1 (2015) 01-05
http://rnlkwc.org

ORIGINAL ARTICLE

Functionalization of GNP with sulphur containing molecules and its catalytic application

Gadadhar Barman[1], Swarnali Maiti[1], and J. Konar Laha[2*]

1. *Department of Chemistry, Midnapore College, Midnapore-721101, W.B, India*
2. *Raja N.L. Khan Women's College, Midnapore-721102, W.B, India*

ARTICLE INFO

Article history

Received 10 October 2015
Accepted 11 November 2015

Keywords:
Gold nanoparticle,
Cysteine,
MPA,
o-nitrophenolate,
o-aminophenolate,
Catalytic reduction

ABSTRACT

In this work, we have synthesized GNP by adopting a green method. Aqueous extract of *Andrographis Paniculata* was used for reduction and stabilization of GNPs and funtionalization of GNPs were done with two biologically relevant molecules containing sulphur such as cysteine and 3-mercaptopropanoic acid (MPA). The GNPs interacted with cysteine and MPA through sulphur atom to produce assembly of nanoparticles of GNPs. The assemblies of the nanoparticles were established using UV-Visible spectra and transmission electron microscopy. The functionalized GNPs have been also utilized to verify the catalytic activity of it by reducing o-nitrophenol to o-aminophenol. The reduction of o-nitrophenol to o-aminophenol is evidenced by a decrease in absorbance at 400 nm and simultaneous growing of a new peak at 296 nm associated with formation of o-aminophenol. The plot of natural log of the absorbance at 400 nm (ln A_{400nm}) versus time produced almost straight line. As the reduction reaction is pseudo-first-order in the presence of excess $NaBH_4$ and catalyst, the slope of the plot mentioned above, yields the apparent reaction rate (k_{app}) 1.5 $\times 10^{-3}$ (s^{-1}) and 5.6×10^{-3} (s^{-1}) for cysteine and MPA functionalized GNP respectively for this trial.

INTRODUCTION

Gold nanoparticles (GNP) are extensively used in various applications including electronics, bio-sensing and surface enhanced Raman spectroscopy. GNPs have found to receive great attention in the progress of optical sensing schemes [1-5]. The SPR band is sensitive to the size and shape of the particles [6]. GNPs smaller than 60 nm in diameter display an intense red color due to SPR absorption when their conducting electrons are confined to dimensions smaller than electron mean free path [7].

Self assembly of nanoparticles is an essential aspect in nanoscience and nanotechnology [8]. A number of chemical strategies have been employed to formulate assemblies of nanoparticles [9,10]. Gold nanorods have been assembled using DNA, surfactants and various linker molecules [11-17]. Development of chains and necklaces of self assembled gold nanopaticles using organic linker molecules would involve two processes: one of them is the interaction of the linker molecules with the gold nanoparticles and the other is the formation of the extended chains or necklaces. When the assembly of GNPs takes place, the color turns blue or purple because of the coupling of the Plasmon absorbance which could results as the nanoparticles come close. Assemblies of nanoparticles are reported as GNPs-based colorimetric recognition of DNA [18,19], proteins [20] and metal ions [21].

***Correspondence to:**

Dr. J. Konar Laha, Principal, Raja N.L. Khan Women's College, Midnapore-721102, W.B, India.
Tel.: +919434029182;
E-mail: j.laha@yahoo.co.in

Catalysis at the nanoscale level has gained significant attention in the past two decades due to the unique properties of materials at that level [22]. Metal nanocatalysts have found a wide range of applications in various field like carbon nanotube nucleation [23], alcohol dehydrogenation [24], oxidation of aromatic alcohol [25], formation of hydrogen peroxide from H_2 and O_2 [26], formic acid electro-oxidation [27], reduction of oxygen [28] etc. Gold, in particular, has become the basis for novel catalysts due to its special activity at the nanoscale [29].

In this work, we have synthesized GNP by adopting a green method. Aqueous extract of *Andrographis Paniculata* was used for reduction and stabilization of GNPs and funtionalization of GNPs were done with two biologically relevant molecules containing sulphur such as cysteine and 3-mercaptopropanoic acid (MPA). The GNPs interacted with cysteine and MPA through sulphur atom to produce assembly of nanoparticles of GNPs. The assemblies of the nanoparticles were established using UV-Visible spectra and transmission electron microscopy. The functionalized GNPs have been utilized to verify the catalytic activity of it by reducing o-nitrophenol to o-aminophenol.

MATERIALS AND METHODS

Chloroauric acid, mercaptopropanoic acid and cysteine, all of A R grade, were purchased from Sigma-Aldrich Chemical Ltd. Sodium hydroxide, was purchased from Merck. Double distilled de-ionized water was used in all experiments.

Andrographis Paniculata was collected from local forest, washed with water and dried under sunlight for one week. It was then crushed into small pieces using mortar pestle. 5 gm of these were taken in a beaker and 100 ml double distilled de-ionized water was poured into it. Then it was kept standing for 6 hours and was filtered to get aqueous extract of *Andrographis Paniculata*. From this extract we prepared diluted extract having different compositions like

5:4 (5 ml extract and 4 ml water), 5:3 (5 ml extract and 3 ml water) and 5:1 (5 ml extract and 1 ml water).

Green synthesis of Gold Nanoparticles by *Andrographis Paniculata* extract

GNP was produced by reduction of chloroauric acid solution using aqueous extract of *Andrographis Paniculata*. 10 ml of aqueous *Andrographis Paniculata* extract of 5:1 composition was cooled in ice cold water and 5 ml of 0.005M aqueous chloroauric acid was added drop wise with continuous stirring. The mixture was then cooled further for 10 minutes and finally it was heated for 30 minutes at 80^0C. The colour of the solution gradually changed from yellow to reddish violet. The reddish violet colour indicated the formation of gold nanoparticles (GNPs).

Functionlization of GNP with Cysteine

10 ml of as prepared GNP was added to 2 ml of alkaline cysteine solution having different concentrations (0.001 to 0.005 M). The mixture was heated at 85^0C for 10 minutes and the color of the sol became reddish violet to violet and finally with increased concentration of cysteine the sol color change to light blue.

Functionlization of GNP with 3-mercaptopropanoic acid (MPA)

10 ml of as prepared GNP was added to 5 ml volume of MPA solution containing different concentrations (0.001 to 0.01 M). The mixture was heated at 85^0C for 5 minutes and the color of the sol became reddish violet to deep blue with increased concentration of MPA.

Functionalized GNP catalyzed reduction of o-nitrophenol

The catalytic reduction of o-nitrophenol to o-aminophenol was carried out in presence of functionalized GNP. A freshly prepared aqueous solution of sodium borohydride (2 ml of 0.005 M) was added in the reaction mixture containing 3 ml functionalized GNPs and 1ml of 0.001 M o-nitrophenol. The colour of the solution changed gradually from yellowish to colourless as the reduction proceeded using either cysteine or MPA functionalized GNP.

The absorbance spectra of the GNPs were analyzed by using a 'SHIMADZU' UV 1800 spectrophotometer and TEM images were taken using JEOL-JEM 2100 high resolution transmission electron microscope (HR-TEM). Samples for the TEM studies were prepared by placing a drop of the aqueous suspension of particles on carbon-coated copper grids followed by solvent evaporation under vacuum. The crystalline nature of the GNPs was examined using X' Pert Pro X-ray diffractometer operated at a voltage of 40 kV and a current of 30 mA with Cu Kα radiation.

RESULTS AND DISCUSSION

The Bio-synthesis of gold nanoparticles using plant extracts are in vogue now-a-days. The use of varied biological systems for the synthesis of gold nanoparticles is evolving different kind of important branches of nanotechnology. The present study deals with the synthesis of gold nanoparticles using a green technique using aqueous extract of *Andrographis Paniculata*.

The GNP produced exhibits reddish violet color in water. The color appears due to the excitation of the Localized Surface Plasmon vibrations of the metal nanoparticles. A smooth and narrow absorption band was observed at 519 nm for the 5:4 extract composition of *Andrographis Paniculata.* The Plasmon band shifted to higher values and becomes broad with the increase of concentration of *Andrographis Paniculata* in the extracts and finally it reaches at 530 nm for 5:1 composition (Fig. 1A). *Andrographis Paniculata* is a strong reducing agent but not a good capping agent. So, this induces rapid nucleation and can't restrict the growth of gold nanoparticles. Hence polydispersed gold nanoparticles are observed. The polydispersity and the colloidal instability (agglomeration tendency of gold nanoparticle) may by the reason of having broad spectrum of gold sol along with a shift in the peak position (Fig. 1A, 5:1 composition). GNP synthesized from *Andrographis Paniculata* extract of 5:1 composition has been used throughout the experiment for colorimetric sensor properties study.

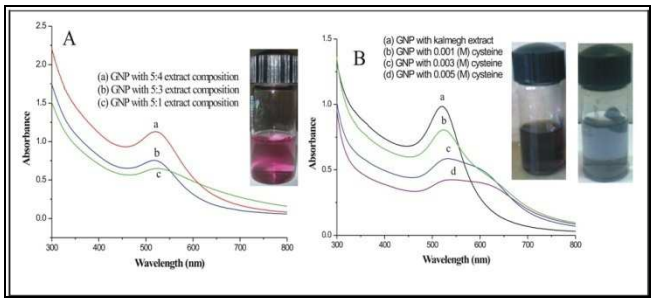

Fig. 1. UV-Vis spectra of (A) GNP at different extract composition, (B) functionalization of GNP with different concentration of cysteine and corresponding digital photographic images of color change (inset).

Functionalization of GNP with cysteine

From the UV-Visible spectra it is observed that the GNP peak becomes broader due to functionalization with cysteine. As the concentration of cysteine increased, the corresponding GNP peak gradually broadened (Fig. 1B). This broadening may be due to the linking of gold particles [30].

Andrographis Paniculata is strong reducing agent but not so good capping agent. So, it induces rapid nucleation and can't restrict the growth of gold nanoparticles. Hence polydispersed gold nanoparticles are observed in TEM micrographs having size in between 10 to 22 nm (Fig. 2A).

Being a strong capping agent, cysteine stabilizes the gold nanoparticles as soon as nucleation happens and there by restricted the nanoparticles to a finite size of 5 to 13 nm (Fig. 2B-D). The presence of linker atom sulphur in cysteine facilitates the binding of the molecules to gold nanoparticles [31]. Due to the electrostatic interaction, assembling processes occur and hence chain or necklace formation of GNP happened through the formation of zwitterions (Scheme 1). The assemblies of nanoparticles are evidenced in transmission electron microscopic images (Fig. 2B-D).
The morphology and the orientation of gold nanoparticles are clearly observed in the TEM images in presence of cysteine (0.005 M). Different geometrical structures like triangular sheets or hexagonal sheets along with chain structures are visible (Fig. 3). The crystalline natures of gold nanoparticles are shown in SAED images (Fig. 3 inset).

Functionalization of GNP with MPA

In presence of MPA the UV-Visible peak of GNP also becomes broader with the increase of the concentration of MPA (Fig. 4). The broadening of the peak may be due to the linking of gold nanoparticles.

3-mercaptopropanoic acid is strong capping agent stabilizes the gold nanoparticles as soon as nucleation happens and there by restricts the nanoparticles to a finite size of 10 to 17 nm were obtained in TEM micrograph (Fig. 5 A and 5B). Simultaneously the linking of molecules facilitates the assembling processes by hydrogen bonding between the carboxylic groups and thereby formation of chains or necklaces occurs (Fig. 5 C and 5D) through the formation of six-member dimeric hydrogen bonded ring (Scheme 1). Formation of such chains or necklaces using organic linker molecules like MPA and cysteine would involve two processes: (i) interaction of the linker molecules with the gold nanoparticles and (ii) formation of the extended chains or necklaces. The attractive chain or necklaces formation occurred in case of MPA functionalized GNP due to the better binding property of MPA molecules with compare to cysteine molecules.

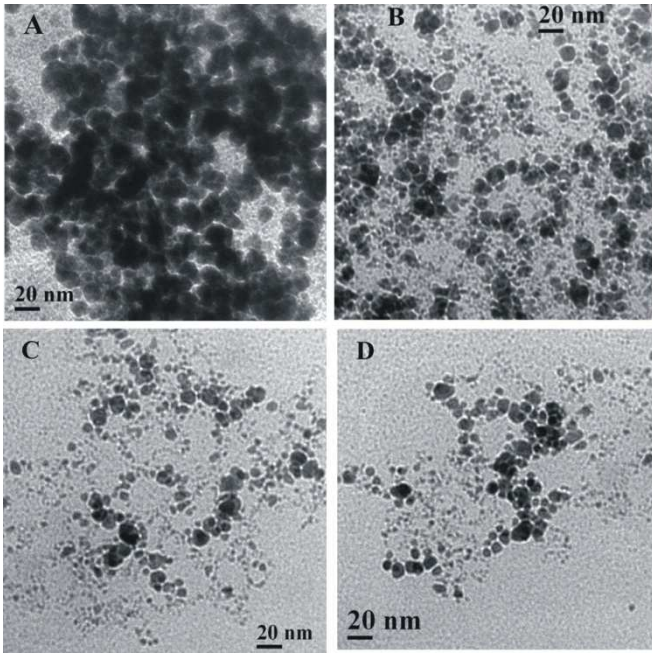

Fig. 2. TEM micrographs of (A) GNP and (B-D) cysteine functionalized GNP synthesized by *Andrographis Paniculata* extract.

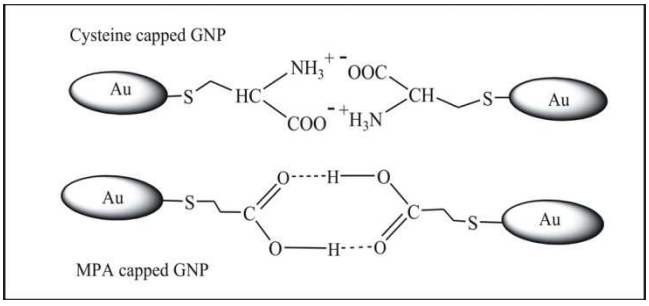

Scheme 1. Strategy of the assembly process and resulting the formation of chain or necklaces type GNP strucrure.

GNP Catalyzed reduction of o-nitrophenol

We have employed the cysteine and MPA functionalized GNP to verify the catalytic activity of it by reducing the o-nitrophenol (Fig. 6). The reduction of o-nitrophenol in the presence of $NaBH_4$ and functionalized GNP is fast. From literature it is confirmed that the role of the metallic catalyst is to bind the o-nitrophenol molecule through the two oxygen atom of the nitro group [32-34].

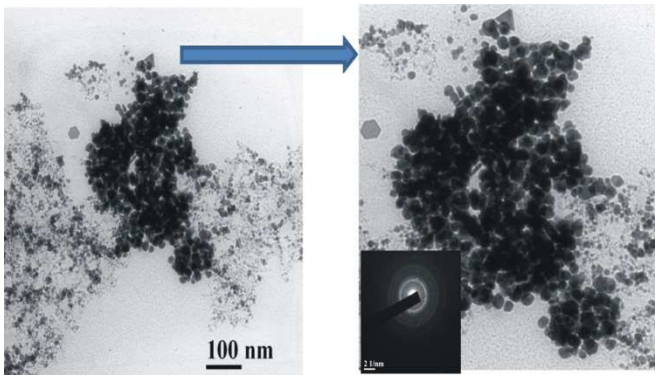

Fig. 3. TEM micrograph of different morphology of cysteine functionalized GNP and the corresponding SAED pattern (inset).

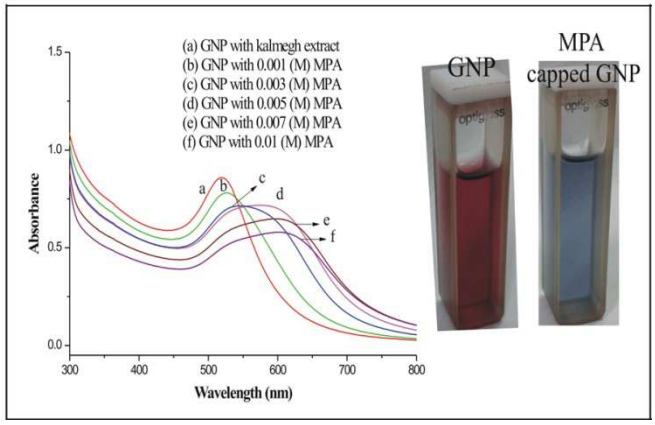

Fig. 4. UV-Vis spectra of MPA functionalized GNP at different concentration of it and corresponding digital photographic images of color change (inset).

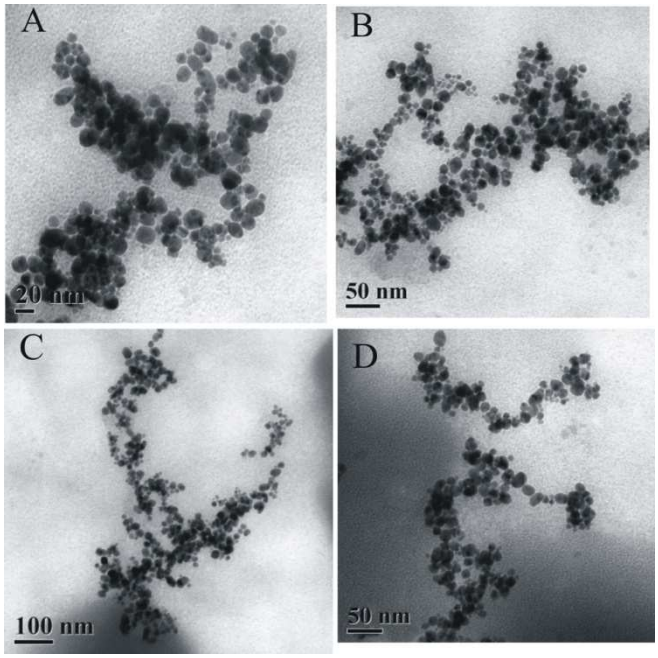

Fig. 5. TEM micrographs of (A-D) MPA functionalized GNP synthesized by *Andrographis Paniculata* extract.

o-nitrophenol absorbs strongly in the visible range with a maximum absorbance at 400 nm. The reduction of o-nitrophenol to o-aminophenol is evidenced by a decrease in absorbance at 400 nm and simultaneous growing of a new peak at 296 nm associated with formation of o-aminophenol. The reduction progress was observed for a period of 480 S (Fig. 6).

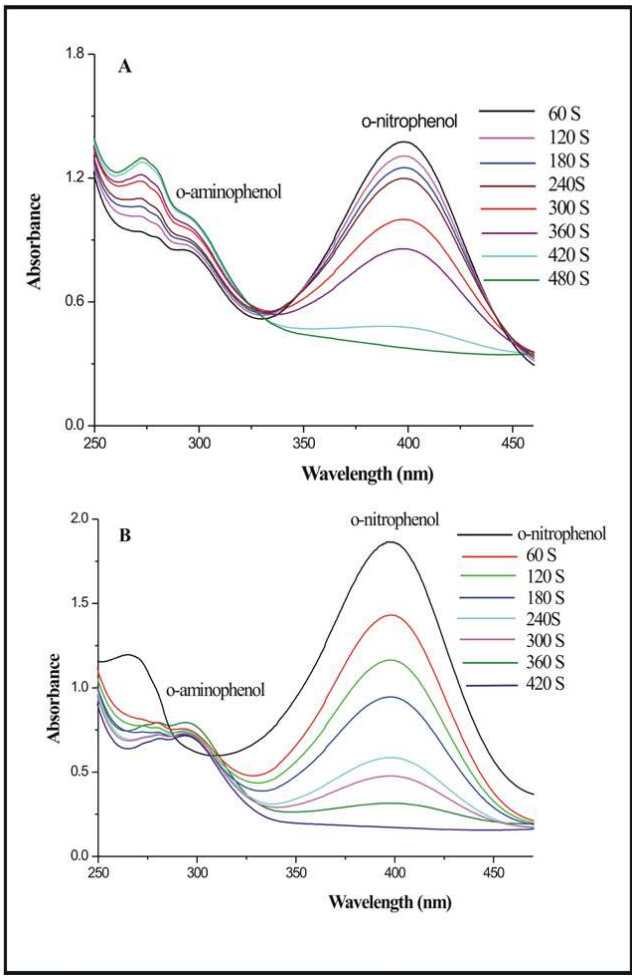

Fig. 6. UV–Visible spectra (A and B) show the reduction progress of o-nitrophenolate using cysteine and MPA functionalized GNP respectively, with time interval of 60 S.

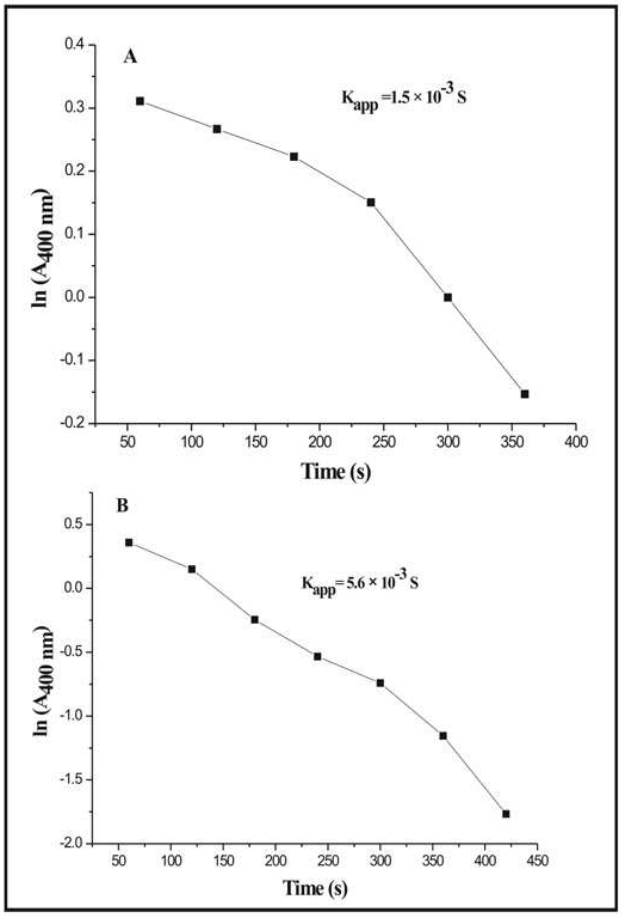

Fig. 7. The plot of the natural log of the absorbance at 400 nm versus time; data points are separated by 60 s intervals. The slope yields the apparent rate constant k_{app} = 1.5 ×10^{-3} (s^{-1}) and 5.6×10^{-3} (s^{-1}) for cysteine and MPA functionalized GNP respectively for this trial.

The plot of natural log of the absorbance at 400 nm (ln A400nm) versus time produced straight lines. As the reduction reaction is pseudo-first-order in the presence of excess NaBH4 and catalyst, the slope of the plot mentioned above, yields the apparent reaction rate, kapp for both the cysteine and MPA functionalized GNP (Fig. 7). Thus, this is found to be an easy method for determining reaction rate by ultraviolet–visible (UV–Vis) spectroscopy [35].

The XRD analysis was performed to confirm the crystalline nature of cysteine functionalized GNP. Various Braggs' diffractions pattern were clearly visible (Fig. 8A). The face centered cubic (fcc) structure of the bulk gold having peaks at 38.24o, 44.42o, 64.64o, 77.78o and 87.73o indicated the presence of corresponding (111), (200), (220), (311) and (222) planes, respectively. The XRD spectrum of the MPA functionalized GNP is shown in Fig. 8B and it is seen that the spectrum shows the same four peaks. On the basis of these Braggs' diffractions, we can say that the functionalized GNP are fcc and essentially crystalline in nature. The (200), (220) and (311) set of lattice planes were observed to be weak and broadened compared to (111) Bragg's diffraction, which indicated that the cysteine and MPA functionalized GNP were (111) oriented.

CONCLUSIONS

The assembly of the GNPs was established using the biologically relevant molecules containing sulphur such as cysteine and MPA. Due to the presence of linker atom sulphur in cysteine which facilitates the binding of the molecules to gold nanoparticles and hence assembling process by electrostatic interaction, resulting the formation of zwitterions. Chains or necklaces formation of GNP occurs through the formation of zwitterions between cysteine molecules. When we have employed 3-mercaptopropanoic acid as the linker molecules wherein the linkage occurs through the formation of six-membered dimeric hydrogen bonded ring between the carboxylic groups which facilitates assembling process of GNP and hence the formation of chains or necklaces occurs. The reduction of o-nitrophenol to o-aminophenol is evidenced by a decrease in absorbance at 400 nm and simultaneous growing of a new peak at 296 nm associated with formation of o-aminophenol. The reduction progress was observed for a period of 480 S. The plot of natural log of the absorbance at 400 nm (ln A_{400nm}) versus time produced almost straight lines. As the reduction reaction is pseudo-first-order in the presence of excess $NaBH_4$ and catalyst, the slope of the plot mentioned above, yields the apparent reaction rate (k_{app}) 1.5 ×10^{-3} (s^{-1}) and 5.6×10^{-3} (s^{-1}) for cysteine and MPA functionalized GNP respectively for this trial.

ACKNOWLEDGEMENTS

We are thankful to Central Research Facility of IIT Kharagpur, India for HR-TEM and XRD measurements.

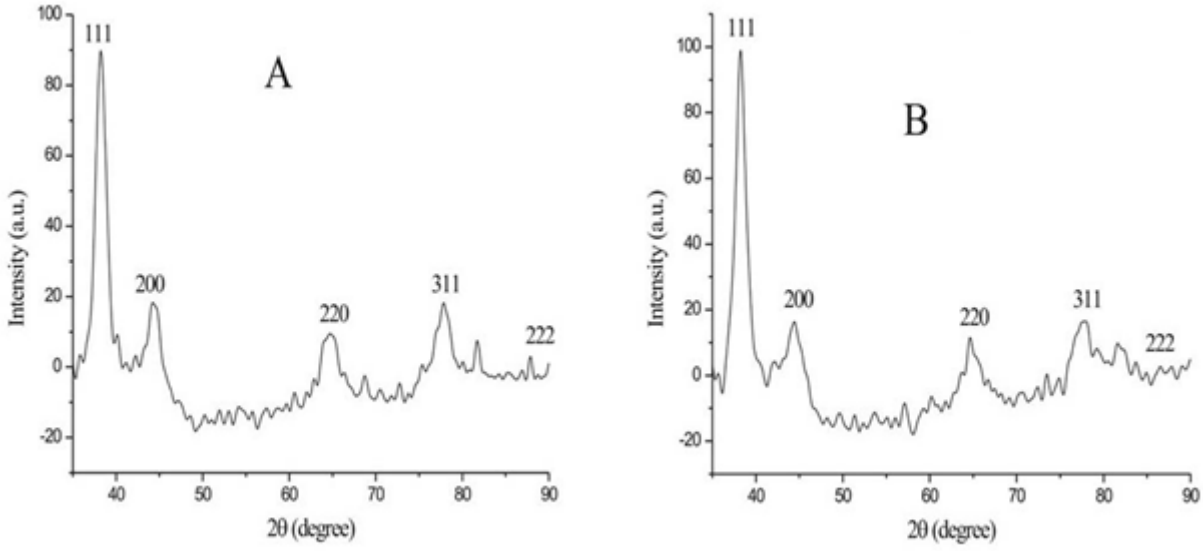

Fig. 8. XRD of (A) cysteine functionalized GNP and (B) MPA functionalized GNP prepared from *Andrographis Paniculata* extract.

REFERENCES

1. Hutter E. and Pileni M.P., 2003, J. Phys. Chem. B, 107, 6497.
2. El-Sayed M.A., 2001, Acc Chem. Res., 34, 257.
3. Barman G., Maiti S. and Laha J.K., 2013, Nanoscale Res. Lett., 8,181.
4. Barman G., Maiti S. and Laha J.K., 2013, J. anal. Sci. Tech., 4, 3.
5. Tokareva I., Minko S., Fendler J.H. and Hutter E., 2004, J. Am. Chem. Soc., 126, 15950.
6. Liu C.W., Huang C.C. and Chang H.T., 2008, Langmuir, 24, 8346.
7. Kim Y.R., Mahajan R.K., Kim J.S. and Kim H., 2010, ACS Appl. Mat. Interfaces, 2, 292.
8. Mbindyo J.K.N., Reisis D., Martin B.R., Keating C.D., Natan M.J. and Mallouk T.E., 2001, Adv. Mat. (Weinheim Germany), 13, 249.
9. Rao C.N.R., Kulkarni G.U., Thomas P.J. and Edwards P.P., 2000, Chem. Soc. Rev., 29, 27.
10. Lyon L.A., Musick M.D. and Nataon M.J., 1998, Anal. Chem., 70, 5177.
11. Dujardin E., Hsin L.B., Wang C.R.C. and Mann S., 2001, Chem. Commun., 14, 1264.
12. Thomas K.G., Barazzouk S., Ipe B.I., Joseph S.T.S. and Kamat P.V., 2004, J. Phys. Chem. B, 108, 13066.
13. Zhang S., Kou X., Yang Z., Shi Q., Stucky G.D., Sun L., Wang J. and Yan C., 2007, Chem. Commun., 47, 1816.
14. Caswell K.K., Wilson J.N., Bunz U.H.F. and Murphy C.J., 2003, J. Am. Chem. Soc. 125, 13914.
15. Joseph S.T.S., Ipe B.I. and Thomas K.G., 2006, J. Phys. Chem. B, 110, 150.
16. Voggu R., Suguna P., Chandrasekaran S. and Rao C.N.R., 2007, Chem. Phys. Lett. 443, 118.
17. Bonifacio A., Sneppen L.V., Gooijer C. and Zwan G.V., 2004, Langmuir, 20, 5858.
18. Elghanian R., Storhoff J.J., Mucic R.C., Letsinger R.L. and Mirkin C.A., 1997, Science, 277, 1078.
19. Mirkin C.A., Letsinger R.L., Mucic R.C. and Storhoff J.J., 1996, Nature, 382, 607.
20. Nam J.M., Park S.J. and Mirkin C.A., 2002, J. Am. Chem. Soc. 124, 3820.
21. Lin S.Y., Chen C.H., Lin M.C. and Hsu H.F., 2005, Anal. Chem. 77, 4821.
22. Toshima N. and Yonezawa T., 1998, New J. Chem., 22, 1179.
23. Ago H., Murata K., Yumura M., Yotani J. and Uemura S., 2003, Appl. Phys. Lett., 82, 811.
24. Mitsudome T., Mikami Y., Funai H., Mizugaki T., Jitsukawa K. and Kaneda K., 2008, Angew Chem., 120, 144–147.
25. Prati L. and Porta F., 2005, Appl. Catalysis A, 291, 199.
26. Hutchings G.J., Carrettin S., Landon P., Edwards J.K., Enache D., Knight D.W., Xu Y.J. and Carley A.F., 2006, Top Catalysis, 38, 223.
27. Waszczuk P., Barnard T.M., Rice C., Masel R.I. and Wieckowski A., 2002, Electrochem. Commun., 4, 599.
28. Vijayaraghavan G. and Stevenson K. J., 2007, Langmuir, 23, 5279.
29. Valden M., Lai X. and Goodman D.W., 1998, Science, 281, 1647.
30. Zhang F.X., Han L., Israel L.B., Daras J.G., Maye M.M., Ly N.K. and Zhong C.J., 2002, Analyst, 127, 462.
31. Varghese N., Vivekchand S.R.C., Gobindaraj A. and Rao C.N.R., 2008, Chem. Phys. Lett., 450, 340.
32. Lv W., Wang Y., Feng W., Qi J., Zhang G., Zhang F. and Fan X., 2011, J. Mater. Chem., 21, 6173.
33. Hammer B., 2006, Top Catalysis, 37, 3.
34. Hallett-Tapleya G.L., Crites C. O.L., Gonzalez-Bejara M., McGilvraya K.L., Netto-Ferreiraa J.C. and Scaianoa J.C., 2011, J. Photochem. Photobiol. A, 224, 8.
35. Zachary D.P., Stacia E.R., Emily K., Kelly T., Wenjie T., Keith J.S. and Graeme H., 2013, J. Phys. Chem. C, 117, 7598.